Molecular Crystals and Liquid Crystals Science and Technology. Section A. Molecular Crystals and Liquid Crystals

Publication details, including instructions for authors and subscription information:
http://www.tandfonline.com/loi/gmcl19

Photoluminescence Studies of C_{60} Single Crystals

J. Feldmann [a], W. Guss [a], U. Lemmer [a], E. O. Göbel [a], C. Taliani [b], H. Mohn [c], W. Müller [c], P. Häussler [c] & H.-U. Ter Meer [c]

[a] Fachbereich Physik and Zentrum für Materialwissenschaften, Philipps-Universität, Renthof 5, 35032, Marburg, Germany

[b] Istituto di Spettroscopia Molecolare, CNR, 40129, Bologna, Italy

[c] Hoechst AG, Angewandte Physik, 65926, Frankfurt, Germany

Version of record first published: 04 Oct 2006.

To cite this article: J. Feldmann , W. Guss , U. Lemmer , E. O. Göbel , C. Taliani , H. Mohn , W. Müller , P. Häussler & H.-U. Ter Meer (1994): Photoluminescence Studies of C_{60} Single Crystals, Molecular Crystals and Liquid Crystals Science and Technology. Section A. Molecular Crystals and Liquid Crystals, 256:1, 757-762

To link to this article: http://dx.doi.org/10.1080/10587259408039321

Mol. Cryst. Liq. Cryst. 1994, Vol. 256, pp. 757–762
Reprints available directly from the publisher
Photocopying permitted by license only

PHOTOLUMINESCENCE STUDIES OF C_{60} SINGLE CRYSTALS

J. FELDMANN[1], W. GUSS[1], U. LEMMER[1], E.O. GÖBEL[1], C. TALIANI[2], H. MOHN[3], W. MÜLLER[3], P. HÄUSSLER[3], H.-U. TER MEER[3]

[1] Fachbereich Physik and Zentrum für Materialwissenschaften, Philipps-Universität, Renthof 5, 35032 Marburg, Germany
[2] Istituto di Spettroscopia Molecolare, CNR, 40129 Bologna, Italy
[3] Hoechst AG, Angewandte Physik, 65926 Frankfurt, Germany

Abstract We present luminescence studies of solid C_{60} for different morphologies such as C_{60} films, polycrystalline C_{60} powder, and C_{60} single crystals. The number of spectrally resolvable peaks is highest for the single crystals as a consequence of reduced inhomogeneous broadening. The fluorescence spectrum of C_{60} single crystals is composed of several defect- or surface-related C_{60} emission centres. The fluorescence lines belonging to each of these so-called X-traps show the characteristic vibronic structure of molecular C_{60} emission, i.e., they reflect the dominant T_{1g}-related false origins.

INTRODUCTION

Since fullerenes have become available in macroscopic quantities, the physical and chemical properties of this novel material system have attracted significant attention. Due to its high symmetry and rigidity, the C_{60} molecule stands out among most other molecules and exhibits characteristic electronic and optical properties. Photoluminescence spectroscopy is one of the most powerful tools to investigate the optical properties of isolated C_{60} molecules and of crystalline C_{60}. Many groups have studied the photoluminescent properties of C_{60} molecules in solution[1,2] and of solid C_{60} in different morphologies such as films, polycrystalline powder,[3–12] and single crystals.[13] However, different optical spectra have been reported even for nominally equal morphologies. Thus, the microscopic interpretation of the fluorescence spectra, in particular for the solid phase, has been controversial up to now. In this paper, we show that the differing optical spectra are a direct consequence of X-trap fluorescence from solid C_{60}.

For all C_{60} systems, fluorescence has been observed covering the spectral range from approximately 650 nm to 1 μm at low excitation intensities. The corresponding fluorescence quantum yields are approximately 10^{-5} for C_{60} in solution and $7 \cdot 10^{-4}$ for solid C_{60}.[2,5] The low quantum yield is a consequence of the long radiative lifetime $\tau_{S_1-S_0}$ of the dipole-forbidden singlet exciton recombination and the fast transfer of excitons from singlet to triplet states (intersystem crossing). Accordingly, the temporal decay of the fluorescence is governed by the time constant $\tau_{S_1-T_1} \approx 1.2$ ns

for the singlet-triplet transfer[14,15] and not by the radiative singlet exciton lifetime $\tau_{S_1-S_0} \approx 1.8\mu s$.

Recently, Negri et al.[16] were able to interpret the vibrational structure of the emission spectrum of *molecular C_{60} in solution.*[2] These authors showed that the fluorescence spectrum can be explained in a Herzberg-Teller scheme, i.e., the lowest singlet excited state T_{1g} acquires ungerade character from energetically higher T_{1u} states by adiabatic vibronic coupling and thus the optical $S_1 - S_0$-transition becomes partially dipole-allowed.[16] As a consequence, so-called false origins determine the peak positions in the fluorescence and absorption spectra of C_{60}. However, only two false origins (209 cm^{-1} separated from each other) originating from t_{1u} and h_u vibronic couplings have appreciable oscillator strengths and are expected to dominate the optical spectra. In addition, Negri et al.[16] showed that the activities of gerade vibronic modes to induce progressions in the fluorescence spectrum are modest (a_g modes) or even negligible (h_g modes).

A comparison of the fluorescence spectra published so far for the various *solid C_{60} systems*[1-13] shows that the shapes of the spectra, peak intensities and even peak positions are not identical for all systems. It therefore seems that interactions of C_{60} molecules with the particular environment influence the luminescent electronic states and/or that distinct chemical impurities themselves contribute to the luminescence spectrum.[6,8] For solid C_{60}, the number of spectrally resolvable peaks obviously depends on the morphology of the C_{60} material.[1-13] Therefore, only high-quality single crystals should allow us (i) to resolve the vibronic structure of the fluorescence spectrum of solid C_{60} and (ii) to understand the influence of defects, surfaces, and impurities on the C_{60} fluorescence spectrum in more detail.

EXPERIMENTAL

C_{60} was produced by the carbon-arc method of Krätschmer and Huffman.[17] The fullerene containing soot was extracted and chromatographically purified by a proprietary process. The C_{60} used is 99.4% pure. This material was sublimed in an inert gas atmosphere to give crystals of $1-2$ mm diameter. The thin films were sublimated from C_{60} in ultra-high vacuum onto quartz substrates. To avoid oxygen contamination all C_{60} samples were kept under Argon atmosphere before mounting them in an evacuated helium flow-cryostat to perform low-temperature luminescence experiments. The excitation photon energy is $2eV$ and we use low excitation intensities of 1 mW focused to a spot size of approximately 100 μm in diameter.

RESULTS

The influence of the morphology of solid C_{60} on the emission spectrum is clearly seen in Fig.1a-c, where normalized fluorescence spectra taken at T=$10K$ are shown for a C_{60} film (a), polycrystalline C_{60} powder (b), and for a C_{60} single crystal (c). The spectrum of the C_{60} film exhibits only two strongly broadened emission bands at approximately 730 nm and 810 nm. It is reasonable in the case of the film to assume that fluorescing C_{60} molecules are located in statistically varying environments leading to pronounced inhomogeneous broadening effects in the optical spectra. The number of resolvable fluorescence peaks drastically increases in the case of the polycrystalline powder and, in particular, for the single crystal. The series of well-resolved luminescence peaks for the single crystal is a consequence of reduced inhomogeneous broadening of the individual optical transitions. At present, it is not clear, whether the linewidth $\Gamma \approx 22$ meV (FWHM) for the fluorescence peaks in Fig.1c is mainly

due to inhomogeneous or homogeneous broadening. However, $\Gamma \approx 22$ meV is an upper limit for the homogeneous linewidth corresponding to a lower limit of 60 fs for the dephasing time $T_2 = 2\hbar/\Gamma_{hom}$. Recently, Brorson et al.[18] performed subpicosecond four-wave mixing experiments on a C_{60} film at low temperature in order to determine the dephasing time. However, they could only give an upper limit of $T_2 \approx 100$ fs. If we assume that the dephasing rate is not sensitive to different C_{60} morphologies, this, together with the linewidth data yields a dephasing time T_2 between 60 fs and 100 fs for the lowest $S_1 - S_0$ transition in solid C_{60} corresponding to a range of the spectral width from 13 meV to 22 meV for the homogeneous linewidth.

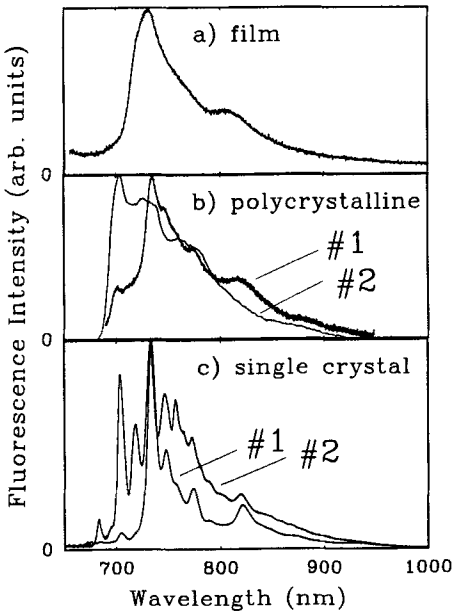

FIGURE 1: Photoluminescence spectra taken at T=10K for different morphologies of solid C_{60}: (a) C_{60} film, (b) polycrystalline C_{60} powder, and (c) C_{60} single crystal. Spectrum #1 of Fig.1b is taken from Ref. [9]. Spectra #1 and #2 of Fig.1c are taken for different positions of the excitation light on the same single crystal.

Spectrum #1 of Fig.1b for polycrystalline C_{60} powder is taken from Ref. [9]. The spectrum peaks at approximately 730 nm and shows a similar but more structured shape than the fluorescence spectrum of the C_{60} film shown in Fig.1a. The fluorescence spectrum of the polycrystalline C_{60} material synthesized as described above is labelled #2 and peaks at approximately 703 nm, i.e., at shorter wavelengths than spectrum #1. In the case of the single crystal we also find differing spectra. The difference between spectrum #1 and spectrum #2 shown in Fig.1c is only the spatial position of the laser excitation spot on the single crystal. This spatially inhomogeneous behavior of the fluorescence spectrum definitely shows that inhomogeneously distributed crystal imperfections such as chemical impurities or crystal defects influence the luminescence process. In a spatial scan over the crystal mostly spectra

similar to the one labelled #1 in Fig.1c are observed. In addition, such a spatial scan shows that a change in intensity for a particular fluorescence line is connected with a simultaneous change in intensity of a spectrally adjacent emission line. In other words, the spectrum seems to be composed of several pairs of emission lines spectrally separated by about 33 meV.

We state that each pair of fluorescence lines originates from C_{60} molecules in a particular crystal environment. The main line at approximately 732 nm is interpreted as fluorescence from C_{60} molecules located in a perfect C_{60} environment, i.e., it stems from bulk C_{60}. Other pairs of peaks are assigned to C_{60} molecules adjacent to chemical impurities, to crystal defects, or to crystal surfaces. The imperfect crystal environment induces an energetic shift of the electronic states and thus of the fluorescence of the particular C_{60} molecule. However, the defect does not change the characteristic vibronic structure of the fluorescence of the adjacent C_{60} host molecule. Such *defect related luminescence from host molecules* are known for anthracene single crystals[19–21] and are called X-traps.

As mentioned, Negri et al.[16] showed that a pair of emission lines corresponding to 1437 cm^{-1} t_{1u}- and 1646 cm^{-1} h_u-related false origins are indeed expected to dominate the fluorescence spectrum of molecular C_{60}. The calculated spectral spacing between these two false origins is 26 meV,[16] whereas the measured fluorescence spectrum of molecular C_{60} in solution provides a spacing of 31 meV[2,16] in good agreement with the observed spacings for the C_{60} single crystal in Fig.1c (as shown below).

A more quantitative analysis of the single crystal fluorescence data is presented in Fig.2. The two spectra of Fig.1c are redrawn in the upper parts. The pair of emission lines at 732 nm and 747 nm are assigned to the t_{1u}- and h_u-related false origins for bulk C_{60} emission. The fluorescence line at 821 nm is interpreted as a 1469 cm^{-1} totally symmetric a_g progression.[3,5,12] In Table 1, the experimental values for the two false origins (t_{1u} and h_u) are listed in the second and third column and in the row labelled C. In addition, the spectral spacing $\Delta \approx 34$ meV between the two experimentally observed t_{1u} and h_u false origins is given in the last column of Table 1. Knowing the spectral positions of the t_{1u} and h_u false origins, the true 0-0 origin can be calculated.[16] We obtain 1.871 eV for the 0-0 origin as listed in the first column of Table 1. This value must be compared to 1.893 eV for C_{60} molecules in solution.[2,16] The minor difference of 22 meV shows that band-structure effects mediated by van der Waals interaction[22] do not cause a pronounced red-shift of the fluorescing excitonic transitions in solid C_{60}.

Three distinct pairs of emission lines corresponding to three distinct C_{60} X-traps are clearly observed when scanning over the single crystal. These X-traps are labelled X_1, X_2, and X_5 in Table 1. The Δ-values for these X-traps are comparable to the one found for bulk C_{60} emission (compare with row C). There seem to be at least two more emission centres in the spectral range around 750 nm. However, their identification is more difficult since the corresponding false origin emission lines overlap. As can be seen in Table 1 we assume two further X-traps X_3 and X_4 to account for the intensity variations around 750 nm. Due to the spectral overlap we cannot directly identify the h_u-related fluorescence lines of the X_3- and X_4-traps from the spectra shown in Fig.2. In order to gain more confidence in our assignment, we have tried to simulate the experimental spectra #1 and #2 shown in the upper parts of Fig.2.

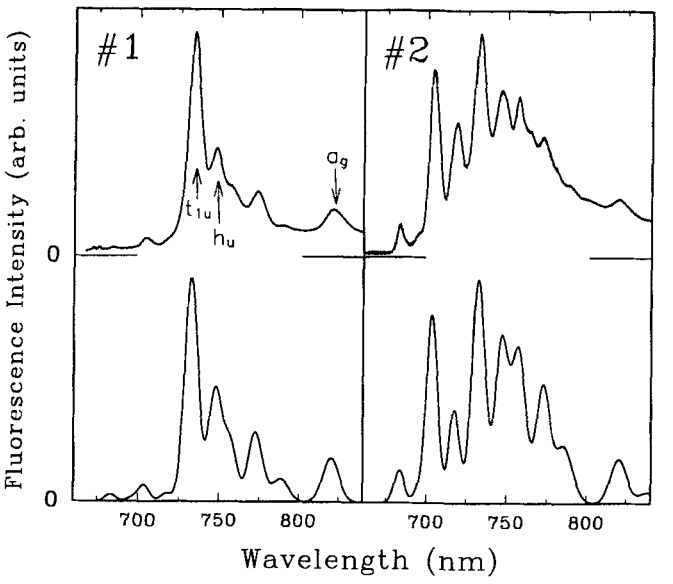

FIGURE 2: Upper part: Same experimental fluorescence spectra as shown in Fig.1c. Lower part: Simulated fluorescence spectrum according to the model described in the text.

	0 - 0	t_{1u}		h_u		Δ
	eV	nm	eV	nm	eV	eV
X_1	1.993	683.2	1.815	695.1	1.784	0.031
X_2	1.940	703.7	1.762	718.4	1.726	0.036
C	1.871	732.4	1.693	747.4	1.659	0.034
X_3	1.839	746.5	1.661	-	-	-
X_4	1.816	757.0	1.638	-	-	-
X_5	1.781	773.5	1.603	789.8	1.570	0.033

TABLE 1: List of emission centres (C: bulk C_{60}, X_i: X-traps). The values for the two false origins, t_{1u} and h_u, are taken from the experimental fluorescence spectra, whereas the true origin 0-0 is calculated using the t_{1u}-frequency from Ref. [16]. Δ is the spectral spacing between the two experimentally determined false origins.

For each emission centre (X_1...X_5,C) listed in Table 1, we assume that only the t_{1u} and h_u false origins and the 1469 cm^{-1} a_g progression contribute to the fluorescence spectrum. For each emission centre, the relative strengths of these three fluorescence

lines are assumed to be 10 : 5 : 2. Taking into account a linewidth broadening of 22 meV for all emission lines, we then superimpose the 'sub-spectra' of all emission centres listed in Table 1. In order to account for the different spectral shapes of spectra #1 and #2, we vary the contribution, i.e., the overall strength of each 'sub-spectrum'. The lower parts of Fig.2 show two calculated fluorescence spectra constructed in such a way.

The main features of the experimentally observed spectra are well reproduced. Fluorescence spectra observed at other crystal positions (not shown in Fig.1 and 2) can also be reproduced using our simple model. Altogether, we find two X-traps (X_1 and X_2) at higher photon energies and three X-traps (X_3-X_5) at lower photon energies as compared to the energetic position of the bulk C_{60} emission (C). The fact that fluorescence from higher energy X-traps (X_1 and X_2) can be observed means that excitation transfer from these X-traps to, e.g., low-energetic bulk C_{60} molecules is hampered at low temperature. We attribute these X-traps at higher energy to surface-related exciton states as is the case for crystalline anthracene.[23] The low-energetic X-traps are most likely due to isolated C_{60} molecules or clusters of C_{60} molecules around a defect.

Our findings demonstrate that the optical properties of crystalline C_{60} exhibit similarities to other molecular crystals and provide a conclusive explanation for the different optical spectra reported so far.

REFERENCES

1. M.R. Wasielewski et al., J. Am. Chem. Soc., 113, 2774 (1991).
2. Y. Wang, J. Phys. Chem., 96, 764 (1992).
3. C. Reber et al., J. Phys. Chem., 95, 2127 (1991).
4. K. Pichler et al., J. Phys. Condens. Matter, 3, 9259 (1991).
5. P.A. Lane et al., Phys. Rev. Lett., 68, 887 (1992).
6. M. Matus, H. Kuzmany, E. Sohmen, Phys. Rev. Lett., 68, 2822 (1992).
7. S.P. Sibley, S.M. Argentine, A.H. Francis, Chem. Phys. Lett., 188, 187 (1992).
8. T. Zhao, J. Liu, Y. Li, and D. Zhu, Appl. Phys. Lett., 61, 1028 (1992).
9. J. Feldmann et al., Europhys. Lett., 20, 553 (1992).
10. H.J. Byrne et al., Appl. Phys., A56, 235 (1993).
11. M. Diehl, J. Degen, H. Schmidtke, Ber. Bunsenges. Phys. Chem., 97, 908 (1993).
12. E. Shin et al., Chem. Phys. Lett., 209, 427 (1993).
13. Y. Iwasa, T. Koda, S. Koda, Synth. Met., 55, 3033 (1993).
14. T.W. Ebbesen, K. Tanigaki, S. Kuroshima, Chem. Phys. Lett., 181, 501 (1991).
15. M. Lee et al., Chem. Phys. Lett., 196, 325 (1992).
16. F. Negri, G. Orlandi, F. Zerbetto, J. Chem. Phys., 97, 6496 (1992).
17. W. Krätschmer et al., Nature, 347, 354 (1990).
18. S.D. Brorson et al., Phys. Rev., B46, 7329 (1992).
19. A. Brillante et al., Chem. Phys. Lett., 31, 215 (1975).
20. V.A. Lisovenko, M.T. Shpak, V.G. Antoniuk, Chem. Phys. Lett., 42, 339 (1976).
21. D.P. Craig and J. Rajikan, J. Chem. Soc., 74, Faraday Transactions II, 292 (1978).
22. S. Saito and A. Oshiyama, Phys. Rev. Lett., 66, 2637 (1991).
23. M.S. Brodin, M.A. Dudinskii, S.V. Marisova, Opt. Spectrosc., 34, 651 (1973).